Technical Note

Measurement of Quasi-Static and Dynamic Displacements of Footbridges Using the Composite Instrument of a Smartstation and an Accelerometer: Case Studies

Jiayong Yu [1, *], Zhen Fang [1], Xiaolin Meng [1,2], Yilin Xie [3] and Qian Fan [4]

[1] Key Laboratory for Wind and Bridge Engineering of Hunan Province, Hunan University, Changsha 410082, Hunan, China; surveying@hnu.edu.cn (J.Y.); fangzhen2@hnu.edu.cn (Z.F.);

[2] Nottingham Geospatial Institute/Sino-UK Geospatial Engineering Centre, The University of Nottingham, Nottingham NG7 2TU, UK; xiaolin.meng@nottingham.ac.uk

[3] Jiangsu Hydraulic Research Institute, Nanjing 210017, Jiangsu, China; xieyilin-1983@163.com

[4] College of Civil Engineering, Fuzhou University, Fuzhou, China; fanqian@fzu.edu.cn

* Correspondence: surveying@hnu.edu.cn

Abstract: Monitoring the dynamic responses of bridge structures has received considerable attention. It is important to synchronously measure both the quasi-static and dynamic displacements of bridge structures. However, the traditional accelerometer method cannot capture the quasi-static displacement component, although it can detect the dynamic displacement component. To this end, a novel composite instrument of a smartstation was proposed to monitor vibration displacements of footbridges. Full-scale experiments were conducted on a footbridge to validate the feasibility of the composite instrument-based monitoring method. A Chebyshev filter and wavelet algorithms were developed to process the composite instrument measurements. It was concluded that the measurement noise of the composite instrument was mainly distributed in a frequency range of 0–0.1 Hz. In two case studies with displacement peaks of 5.7–10.0 mm and 1.3–2.5 mm, the composite instrument accurately identified the quasi-static and dynamic displacements. The composite instrument will be a potential tool for monitoring structural dynamics because of its enhanced overall performance.

Keywords: composite instrument of a smartstation; accelerometer; dynamic displacement; vibration frequency; structural health monitoring

1. Introduction

The measurement of three-dimensional quasi-static and dynamic displacements of bridge structures is an important task for monitoring their structural health [1]. Vibration displacements of bridge structures are usually measured by traditional methods such as the Global Navigation Satellite System (GNSS) and an accelerometer. GNSS technologies are capable of identifying dynamic displacement components (instantaneous deformation) at millimeter-level accuracy with a sampling rate up to 20 Hz, even 100 Hz [2,3]. However, when they are used to identify quasi-static displacement components induced by temperature changes or vehicle loads, their measurement accuracies are limited within a relatively low range from 10 to 20 mm because of multipath signal errors [4,5]. Moreover, although the accelerometer is capable of accurately detecting dynamic displacements of bridges by double integration of the accelerations, it cannot detect quasi-static displacements of bridges because of drift errors when the excitation term is relatively longer [6,7].

In order to solve the above-mentioned problem, a composite instrument of a smartstation was proposed to synchronously monitor both the dynamic and quasi-static displacements of bridge structures. The composite instrument combines a high-performance robotic total station (RTS), which

45 is also called terrestrial positioning system (TPS), and a powerful GNSS unit in one instrument. The
46 GNSS unit is fully integrated into the RTS, rather than a simple combination of two sensors.
47   The greatest advantage of the composite instrument of the smartstation is that it can accurately
48 capture not only three-dimensional coordinates of the monitored target, but also the Global
49 Positioning System (GPS) time information with nanosecond-level accuracy. The GPS time
50 information is very important for multi-sensor data fusion. A prototype of the smartstation system
51 was designed and developed for the first time by Ingensand et al. in 1993. The invention involved a
52 terrestrial surveying system comprising an electro-optic total station for the combined measurement
53 of angle and distance, a connection, and a receiver for a satellite position-measuring system [8]. In
54 order to evaluate the composite instrument of the smartstation, a case survey was conducted on the
55 Porte Palatine, an archaeological building site in Turin. The composite instrument-based technique
56 was considered to be a valuable solution for surveying cultural heritage [9]. The technique has been
57 widely employed in many survey scenarios such as topography, boundary, construction site stakeout
58 and utilities surveys [10].
59   The composite instrument was used to monitor the dynamic responses of a bridge structure in
60 this study. A Leica TCA2003 RTS instrument has been used to monitor the structural dynamic
61 responses of the Wilford Suspension Bridge in Nottingham, UK. However, very little movement of
62 the bridge was measured due to the instrument's slow data sampling-rate of 1 Hz [11]. Ambient
63 vibration measurements of the Bosphorus Suspension Bridge in Turkey were conducted using a TCA
64 2003 RTS instrument [12]. Seven vertical and lateral frequencies were detected from the RTS
65 measurements, which were in the frequency range of 0–0.5 Hz. A new generation Leica 1201 RTS
66 with a nominal sampling-rate of 10 Hz was used to monitor the dynamic responses of the
67 Gorgopotamos Railway Bridge in Greece in response to passing trains [13,14]. The vertical
68 displacements of the bridge with peaks of 2.5 to 6 mm, and its dominant frequencies, which were
69 distributed in a frequency range of 3.18–3.63 Hz, were successfully identified [13,14]. The collocated
70 sensors consisting of RTS, GNSS and an accelerometer were adopted to measure displacements in a
71 stiff footbridge in Greece, and were found to be capable of measuring three-dimensional
72 displacements with amplitudes of a few millimeters and identifying oscillation frequencies [15]. To
73 overcome the RTS shortcoming of its low data sampling-rate, two approaches have been presented
74 to increase the RTS sampling-rate from 10 Hz to 20 Hz to determine the vertical displacements of
75 bridges [16]. It was concluded that the geodetic instruments, GNSS and RTS, in combination with
76 accelerometers can be safely used to measure the semi-static and dynamic deflections of stiff bridges
77 [17]. It is believed that the composite instrument of the smartstation will show better overall
78 performance than the RTS because of its updated hardware and software [10].
79   The focus of this case study is on verifying the feasibility of using the composite instrument to
80 monitor bridge dynamic responses. Background noise in three directions in composite instrument
81 measurements were obtained and analyzed in both time and frequency domains for the purpose of
82 characterizing the smartstation measurement noise. The composite instrument was used to monitor
83 the dynamic responses of the studied footbridge, which were induced by a group of three people
84 jumping, and a gentle wind and occasional pedestrians. The quasi-static and dynamic displacements
85 of the footbridge were accurately detected by the composite instrument.

2. Instrumentation and the Studied Footbridge

2.1. Composite Instrument of the Smartstation

88   The composite instrument of the smartstation (Figure 1) was employed to monitor the dynamic
89 deformation of the footbridge used in this study. The composite instrument combines a high-
90 performance Leica TS30 robotic total station (RTS), which is also called a terrestrial positioning
91 system, TPS), and a powerful Leica ATX1230+ GNSS smart-antenna in one instrument. The GNSS
92 unit is fully integrated into the RTS. All data are stored in the same database on the same
93 CompactFlash card, all GNSS and RTS operations are controlled via the RTK keyboard with the entire

94   software in the RTS, and all measurements, status and other information are displayed on the RTS
95   screen (Figure 1).
96   The composite instrument has the capability of automatic target recognition (ATR), which
97   allows fast, dynamic tracking of targets in three dimensions. The composite instrument can obtain
98   three-dimensional coordinates of a prism with a true sample-rate of up to 5–7 Hz, as well as the
99   nanosecond-level GPS time information in each record. The nominal sampling-rate of the composite
100   instrument of the smartstation is 10 Hz. However, the true sampling-rate of the instrument is 5–7 Hz
101   became of missing data. The composite instrument is one of the best performing coordinate
102   measurement instruments, with a nominal angle accuracy of ± 0.5″ and a nominal distance accuracy
103   of 0.6 mm + 1 ppm.

104
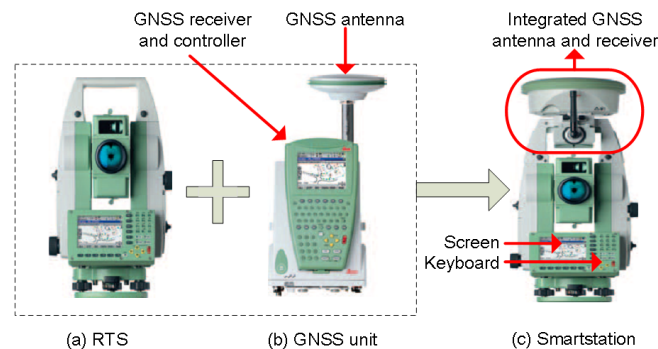
105   **Figure 1.** The composite instrument of the smartstation. The composite instrument combines a high-
106   performance Leica TS30 robotic total station (RTS) (a) and a powerful Leica GNSS unit (b) in one
107   instrument.

108   *2.2 Accelerometer and Precise Time Data Logger*

109   A Kistler 8392A2 triaxial accelerometer with a data sample-rate of 150 Hz was used to monitor
110   the bridge dynamic responses to verify the results from the composite instrument. It is ideal for modal
111   tests of large structures, with technical parameters in the acceleration range of 2 g, a sensitivity of 500
112   mV/g, resolution of 0.3 mg and a weight of 40 g. For the purpose of solving the problem of time
113   synchronization, a precise time data logger (PTDL) was applied to record the accelerator data (Figure
114   2c). It can tag the GPS time onto the external data from the accelerometer because it contains a built-
115   in, low-cost GPS chip and a small antenna [18]. Thus, the data from both the composite instrument
116   and the accelerator can be applied for data fusion or comparison based on the same GPS time system.

117   *2.3 Description of the Nottingham Wilford Suspension Bridge*

118   Full-scale experiments were performed on the Wilford Suspension Bridge in Nottingham, UK
119   (Figure 2a). The bridge, which is also known as the Meadows Suspension Bridge, is a combined
120   suspension pedestrian footbridge and aqueduct that crosses the River Trent, linking the town of West
121   Bridgford to the Meadows. The historical bridge was constructed in 1904 with a 69.0-m-length main
122   span. Following a restoration in 1983, it was closed to pedestrians in 2008 for a major restoration
123   because of debris falling from the bridge deck. In the last two decades, the bridge has been utilized
124   as the testbed for the purpose of monitoring research with innovative sensors and approaches. The
125   first three modal frequencies of the bridge, i.e., 1.44 Hz, 2.79 Hz and 4.66 Hz, have been computed
126   with its finite element model in previous research [19]. The modal parameters of the bridge might
127   have changed due to the major restoration in 2008.

128

129
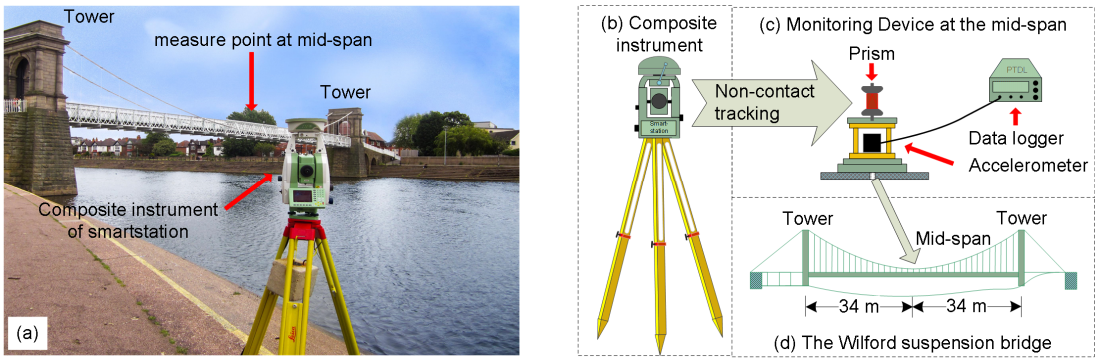
Figure 2. The Wilford Suspension Bridge in Nottingham and the instrumentation. The composite instrument was set near the bridge to monitor the structural dynamic response (a); the composite instrument (b) in non-contact mode locked and tracked a 360° prism that was installed outside a cage with a triaxial accelerometer, connected to a precise time data logger (c); the monitoring devices were fixed at the mid-span of the footbridge for dynamic response monitoring (d).

135

Table 1. The details of the three experimental cases.

Case	GPS time	Description	Instrumentation
1	From second 314,100 to 314,700, GPS week 1768	Measuring background noise in measurements of the composite instrument	A composite instrument of the smartstation
2	From second 312,500 to 313,700, GPS week 1698	Measuring three people jumping - induced vibrations of the footbridge	A composite instrument and a tri-axial accelerometer
3	From second 476,100 to 477,300, GPS week 1699	Measuring gentle wind and occasional pedestrian-induced vibrations of the footbridge	A composite instrument and a tri-axial accelerometer

3. Methodology for the Field Measurements

Three experiments with different working conditions were performed in this study (Table 1). Before the full-scale experiments were undertaken, a static experiment (Case 1) was carried out on the campus of the University of Nottingham to understand the noise characteristics in the measurements of the composite instrument. The two full-scale experiments were conducted on the Wilford suspension bridge in Nottingham to verify the measurement of the vibration displacement of footbridges using the composite instrument (Figure 2). In case 2 and 3, the vibration displacement of the footbridge was monitored by the composite instrument, with the displacement being induced by three people jumping, and gentle wind and an occasional pedestrian (Case 3). The vibration displacements cover both the quasi-static and dynamic displacement components.

In the static experiment (Case 1), the composite instrument and the prism were each mounted on a tripod. The two tripods were setup on two stable sites on the campus of the University of Nottingham, with a distance of 60 m between the two tripods. The 3D coordinates of the prism were measured and recorded continuously by the composite instrument with a true sample-rate of 5~7 Hz. A three-axis coordinate system was constructed with the x-axis aligned with the measuring direction from the composite instrument to the prism, and the z-axis was coincident with the gravity direction. Because the prism is not moving, any displacements found in the composite instrument observations can be regarded as background noise [20,21]. We acquired the background noise in three directions over about 60 min. We graphically analyzed a 600-second-long displacement time series from 314,100 seconds to 314,700 seconds, GPS week 1768.

In the full-scale experiment (Case 2), the composite instrument station was set up on stable site A2, located at the downstream side of the footbridge, 67.2 m away from the measuring point at the

mid-span of the footbridge (Figure 3). The composite instrument acquired vibration displacement at the measuring point with a true sample-rate of 5–7 Hz. The backsight point of the composite instrument was set at the upstream (north) side of the studied bridge, approximately 74.8 m away from the corresponding instrument station. It is necessary to choose the right site as the backsight point because of the need for a line-of-sight between the backsight point and the instrument station. The measuring point was set at the midspan of the footbridge. Monitoring devices were installed at the measuring point of the midspan, including a Leica GRZ122 360° prism, a Kistler 8392A2 triaxial accelerometer, a PTDL data logger produced by the research team at the University of Nottingham, and a special cage. The special cage was fixed on the rail of the midspan of the footbridge. The accelerometer was fixed inside the cage whereas the prism was installed outside the cage (Figure 2c). The PTDL data logger was adopted to record the accelerometer data in the GPS time system, with a data sampling-rate of 100 Hz.

The forced vibrations of the footbridge were monitored by both the composite instrument and accelerometer sensors, which were induced by three people jumping simultaneously at the midspan for several minutes. We acquired both displacement and acceleration time series from 312,500 seconds to 313,700 seconds, GPS week 1698.

In the full-scale experiment (Case 3), the instrument station was located at the A3 site, 64.4 m away from the measuring point of the footbridge (Figure 3). Similar to the previous case, the vibration responses of the footbridge were measured by both the composite instrument and accelerometer sensors, which were induced by a gentle wind and an occasional pedestrian. We synchronously acquired one set of 1200-second-long displacement time series with a data sampling-rate of 5-7 Hz, and one set of 1200-second-long acceleration time series with a data sampling-rate of 100 Hz, from 476,100 seconds to 477300 seconds, GPS week 1699.
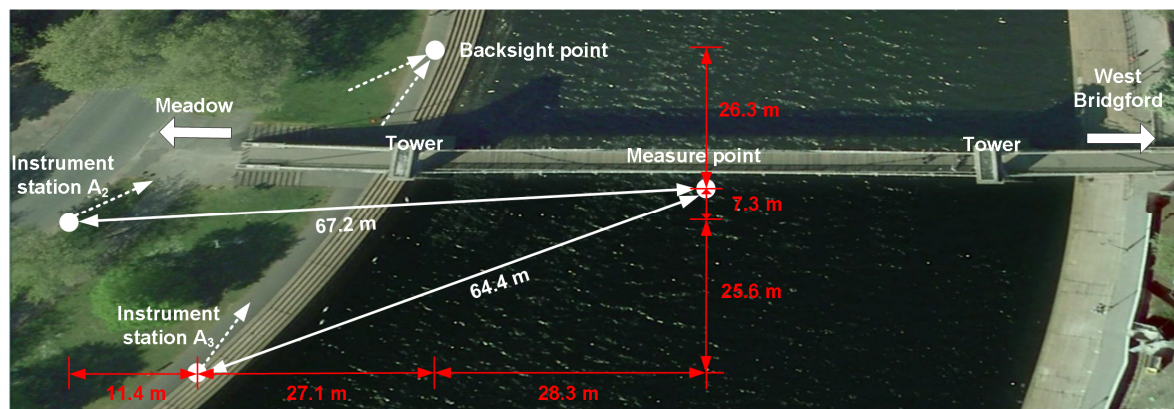
Figure 3. Instrument layout of full-scale experiments performed on the Wilford Suspension Bridge. The instrument stations for the composite instrument were set at the A2 and A3 sites in Cases 2 and 3, respectively. The backsight point was set at the upstream (north) side of the bridge; the measuring point was set at the mid-span of the studied footbridge.

4. Results and Discussion

The background noise in the measurements of the composite instrument were detailed in both time and frequency domains by the continuous Morlet wavelet transform (CMWT) algorithm. The dynamic responses of the footbridge were induced by a group of three people jumping, and gentle wind and the occasional pedestrian. The two cases were monitored and identified by the composite instrument.

4.1. Background Noise in the Composite-Instrument Measurements

In order to characterize the measurement noise of the composite instrument in detail, a set of displacement time series in three directions were acquired by the composite instrument in the static experiment of Case 1. The displacement in each record included the point number, GPS time, x-coordinate, y-coordinate and z-coordinate. A standardized identification procedure was used to

197　preliminarily process these original records for the purpose of removing duplicates and outliers,
198　recovering missing records, and so on [21]. Firstly, the duplicate records with an identical recording
199　time were removed from the original records; these were caused by the high data-recording rate of
200　the composite instrument. Secondly, the outliers were removed from the original displacement
201　records according to a threshold of three times the standard deviation. Finally, the missing records
202　were recovered by a linear interpolation method according to a time interval of 0.1 s between two
203　adjacent records. The MATLAB codes were developed to preliminarily process those original records
204　with the above methods by the authors.

205　　Figure 4 graphically depicts the profile of the background noise in the measurements of the
206　composite instrument in three directions when the composite instrument is 60 m away from the
207　prism. The displacement in the x-axis are primarily caused by the x-axis being parallel with the
208　sighting-distance direction, which shows the resolution of the distance meter. The y- and z-axes noise
209　is caused by both angle and distance errors because they are determined by the distance and their
210　corresponding angles. The amplitude of the background noise fluctuates between -1.4 mm and 0.6
211　mm in the x-axis, between -0.9 mm and 1.0 mm in the y-axis, and between -1.1 mm and 0.8 mm in the
212　z-axis (vertical direction). In the horizontal plane, the x-axis is coincident with the sighting line of the
213　composite instrument whereas the y-axis is perpendicular to the sighting line. All standard
214　deviations (SD) and mean absolute errors (MAE) of the background noise in each direction are less
215　than 0.5 mm (Table 2). The results show that the measurement accuracies of the composite instrument
216　monitoring technique meet the requirements for monitoring the dynamic deformation of footbridges.

217　　Figure 5 graphically depicts the frequency domain characteristics of the composite instrument
218　measurement noise, which correspond to the displacements shown in Figure 4. The spectra of
219　background noise in three directions were produced using the CMWT algorithm (seeing details in
220　references [22, 23]).

221
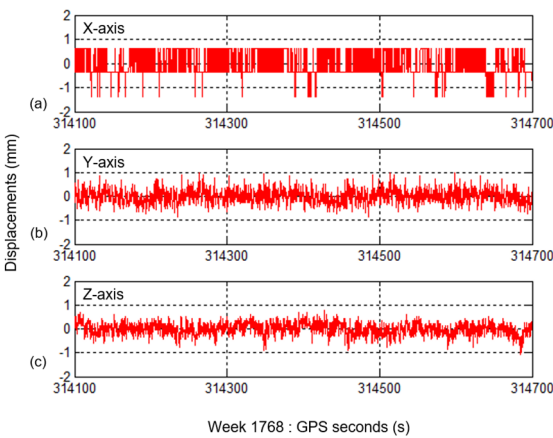
222　**Figure 4.** Time history of the background noise in the composite instrument measurements in
223　experimental Case 1. The prism was set up on a stable site, 60 m away from the composite instrument.

224　**Table 2.** Standard deviations (SD) and mean absolute errors (MAE) of background noise in the
225　composite instrument measurements.

Direction	SD (mm)	MAE (mm)
x-axis	0.5	0.4
y- axis	0.3	0.2
z- axis	0.2	0.2

226　　It is noted that the noise is mainly distributed in a frequency range of no more than 0.1 Hz, and
227　is caused by the angle and distance measurement errors of the composite instrument. The noise
228　energy in a frequency range of more than 0.1 Hz is relatively low, and is mainly caused by instrument
229　self-noise such as Gaussian noise and white noise [24]. Besides, it is obvious that the noise energy in

230 the z-axis is lower than that in the x- and y-axes. This characteristic agrees well with the SD and MAE
231 values for the background noise in the composite instrument measurements, as shown in Table 2.
232 The accuracies of the horizontal displacements are determined by the horizontal-angle and distance
233 measurements, and the accuracies of vertical displacements are determined by the vertical-angle and
234 distance measurements. Horizontal angle accuracies are usually lower than vertical angle accuracies
235 because the horizontal angle measurements need a horizontal orientation angle. This results in the
236 displacement measurement accuracies in the z-axis direction (vertical direction) being relatively
237 higher than those in the other directions.

238
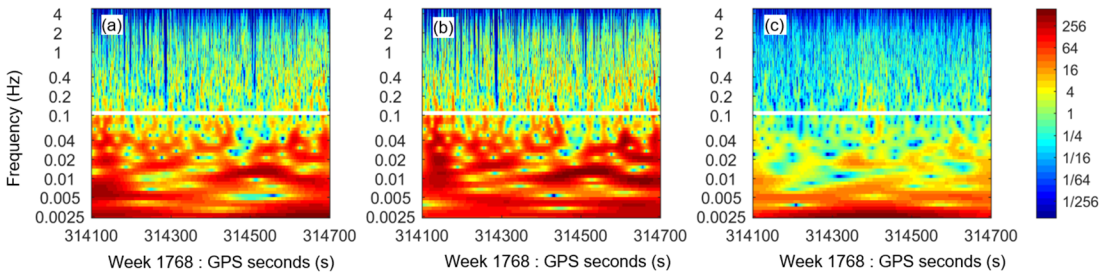
239 **Figure 5.** The continuous Morlet wavelet transform (CMWT)-based spectra of the measurement
240 noise of the composite instrument in the x-axis (**a**), y-axis (**b**) and z-axis (**c**), corresponding to
241 displacement time series in Figure 4 with white lines indicating the frequency of 0.1 Hz. The
242 horizontal axis indicates the GPS time, which is composed of GPS weeks and week seconds. The color
243 pattern indicates the amplitudes of the energy spectrum that are dimensionless.

244 *4.2. Three People Jumping-Induced Vibrations*

245 In experimental Case 2, both the composite instrument and accelerometer sensors were used to
246 monitor the dynamic responses of the Wilford Suspension Bridge, which were induced by a group
247 of three people synchronously jumping for around 10 s each time on its midspan. A set of 1200 s
248 displacement time series with an interval of 0.1 s were acquired by the composite instrument. Also,
249 a set of 1200 s acceleration time series were acquired with an interval of 0.01 s by the accelerometer
250 in the same GPS time frame. Using codes written by the authors, these two groups of time series were
251 preliminarily processed to remove duplicates and outliers, and recover missing records, as in the
252 previous case.
253 Figures 6a-b. graphically depict the overall vibration displacements of the footbridge in the
254 longitudinal and lateral directions measured by the composite instrument. Although the vibration
255 displacements of the footbridge are very small in both the longitudinal and lateral directions, they
256 are accurately measured by the composite instrument. The longitudinal displacements change
257 between -1.3 mm and 1.0 mm with a SD of 0.3 mm. The lateral displacements change between -1.7
258 mm and 1.6 mm, with a SD of 0.5 mm. Figure 6c graphically depicts the vibration displacements of
259 the footbridge in the vertical direction, measured by the composite instrument. Five significant
260 displacement peaks in the vertical direction correspond to the five times that three people jumped at
261 the midspan of the footbridge.
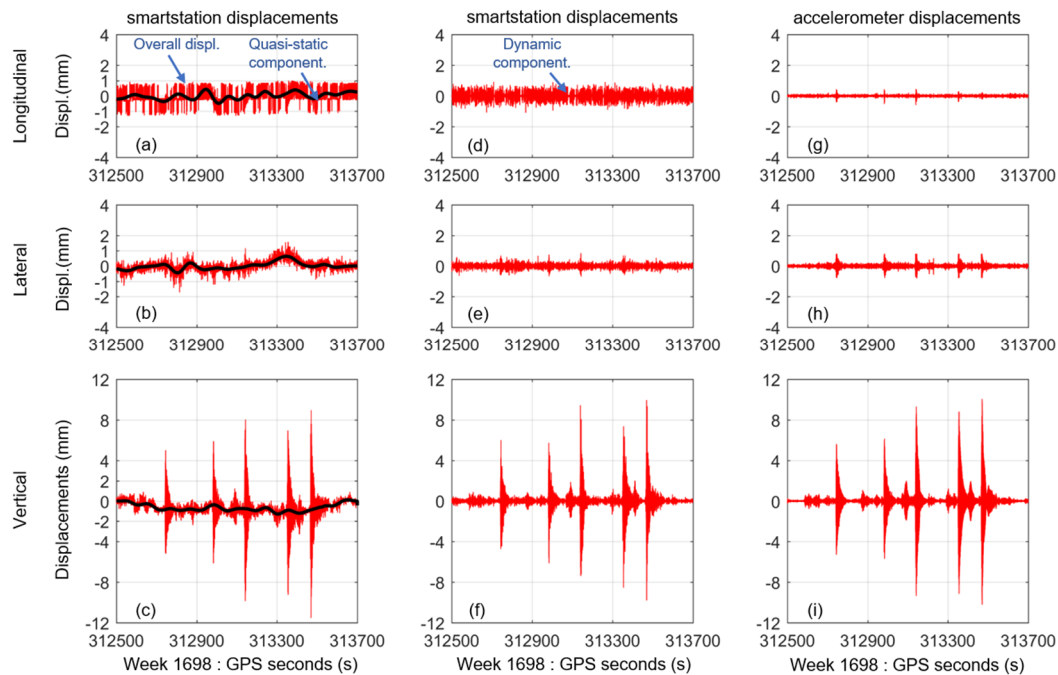
Figure 6. Displacement time series of the footbridge in the longitudinal, lateral and vertical direction induced by a group of three people jumping in experimental Case 2. The vibration displacements of the footbridge measured by the composite instrument (the red curves in the left column) were separated into two parts, i.e., the quasi-static displacements (the black curves in the left column) and the dynamic displacements (central column). The dynamic displacements were also computed from the accelerometer measurements by double integration (right column).

The smartstation-measured vibration displacement of the footbridge were separated into two components, i.e., quasi-static displacements and dynamic displacements using the Chebyshev high pass filter [25, 26]. Also, the dynamic displacements of the footbridge (see right column of Figure 6) were computed from the accelerometer data by double integration [6, 27], and these were used to validate the composite instrument results. It is known that the quasi-static displacements of the footbridge cannot be derived from the accelerometer data because of the trend errors [28].

Although all quasi-static displacements of the footbridge in three directions have low amplitudes of about 1 mm (see the black curves in the left column of Figure 6), the composite instrument can accurately detect these quasi-static displacement components. This suggests that measurement errors of the composite instrument should be lower than a millimeter. The curve of the vertical quasi-static displacements shows a strong correlation between the vertical deflections and experimenter loads (Figure 6c). When three people walked onto the bridge in the first tens of seconds of the experiment, the curve of the vertical quasi-static displacements shows a gradual downward tendency. When three people stay on the midspan of the footbridge, the vertical quasi-static displacements fluctuate close to one millimeter. when three people walk off the footbridge at the end of the experiment, the vertical quasi-static displacements recover to a zero value.

Two sets of dynamic displacements of the footbridge were derived from the composite instrument and the accelerometer data (see the center and right columns of Figure 6). It is obvious that they are similar to each other in each direction. In both the longitudinal and lateral directions, the dynamic displacements have small amplitudes of less than 0.5 millimeters. The measurement errors of the composite instrument should be lower than a half-millimeter. The dynamic displacements computed from the accelerometer data have relatively lower amplitudes than the ones computed from the composite instrument data. The main reason for this is that the random noise of accelerometer data is partly eliminated when the displacements are computed from the accelerations.

In the vertical direction, both two sets of dynamic displacements as shown in Figures 6f and 6i depict five significant peaks, which correspond to the five times that three people jumped on the

295   bridge. The corresponding peak differences between these two sets of dynamic displacements are
296   less than 1.0 mm and the peak difference ratios are no more than 10.0 % (Table 3). This shows that
297   the composite instrument can accurately measure dynamic displacements of the footbridge with peak
298   values of several millimeters (from 5.7 mm to 10.0 mm).

299   **Table 3.** Comparison of peak values of two sets of dynamic displacement in the vertical direction
300   derived from the composite instrument and accelerometer measurements in Case 2.

Event	Peak displacements (mm)		Diff. (mm) (①-②)	Ratio (%) (｜①-②｜)/②
	Composite instrument①	Accelerometer②		
1	**6.0**	5.6	0.4	7.1
2	5.7	6.1	-0.4	6.6
3	9.5	9.3	0.2	2.2
4	7.7	8.6	-0.9	10.5
5	10.0	10.1	-0.1	1.0

301   Figure 7 depicts three pairs of wavelet-based spectra for the overall vibration displacements and
302   dynamic displacements derived from the composite instrument data, and the dynamic displacements
303   derived from the accelerometer measurements in the vertical direction. These wavelet-based spectra
304   provide the local characteristics for the displacement time series. Each three-dimensional spectrum
305   shows five significant displacement peaks, corresponding to the five times that three people jumped
306   at the midspan of the footbridge. The three-dimensional spectrum of the overall vibration
307   displacements shows significant differences with the other two three-dimensional spectra of the
308   dynamic displacements. The reason is that the overall vibration displacements covers relatively
309   higher random noise and quasi-static displacement components. This is similar to the two spectra of
310   dynamic displacements derived from the composite instrument and accelerometer data.

311
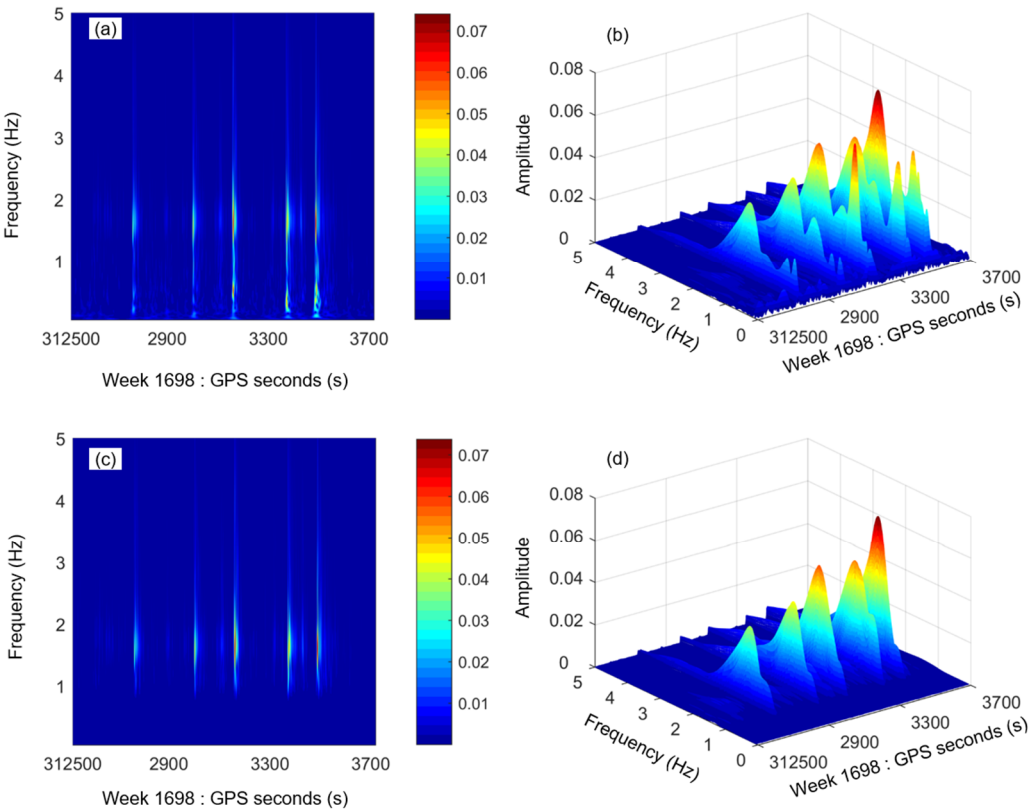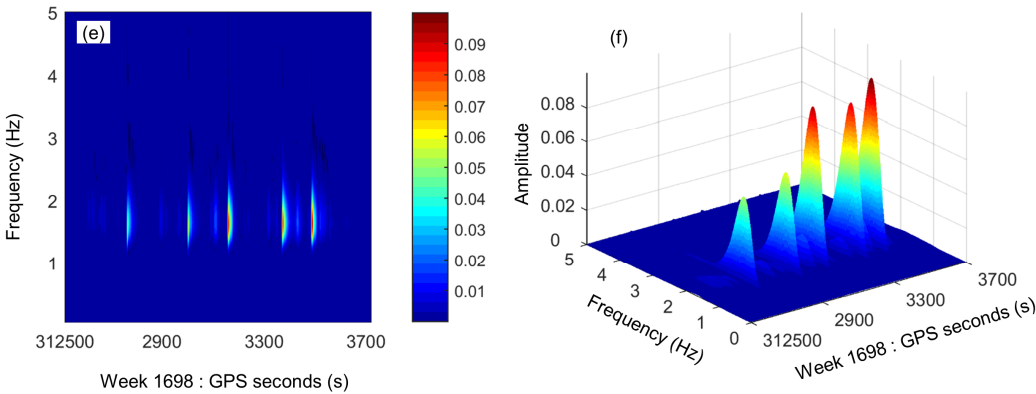
Figure 7. Wavelet-based spectra of the displacement time series in the vertical direction: two- and three-dimensional spectra of overall vibration displacements (**a**, **b**) and dynamic displacements (**c**, **d**) derived from the composite instrument data, and dynamic displacements (**e**, **f**) derived from the accelerometer data. The horizontal axis indicates the GPS time, which is composed of GPS weeks and week seconds. The color pattern indicates the amplitudes of the energy spectrum that are dimensionless.

4.3. Wind and Occasional Pedestrian-Induced Vibrations

The vibration responses of the footbridge, which were induced by gentle wind and occasional pedestrians, were monitored in experimental Case 3. We synchronously acquired 1200-second vibration displacements of the footbridge using the composite instrument, and 1200-second accelerations using the accelerometer in the same GPS time frame. The composite instrument acquired data with a true sampling-rate of 5–7 Hz whereas the accelerometer acquired data with a sample-rate of 100 Hz.
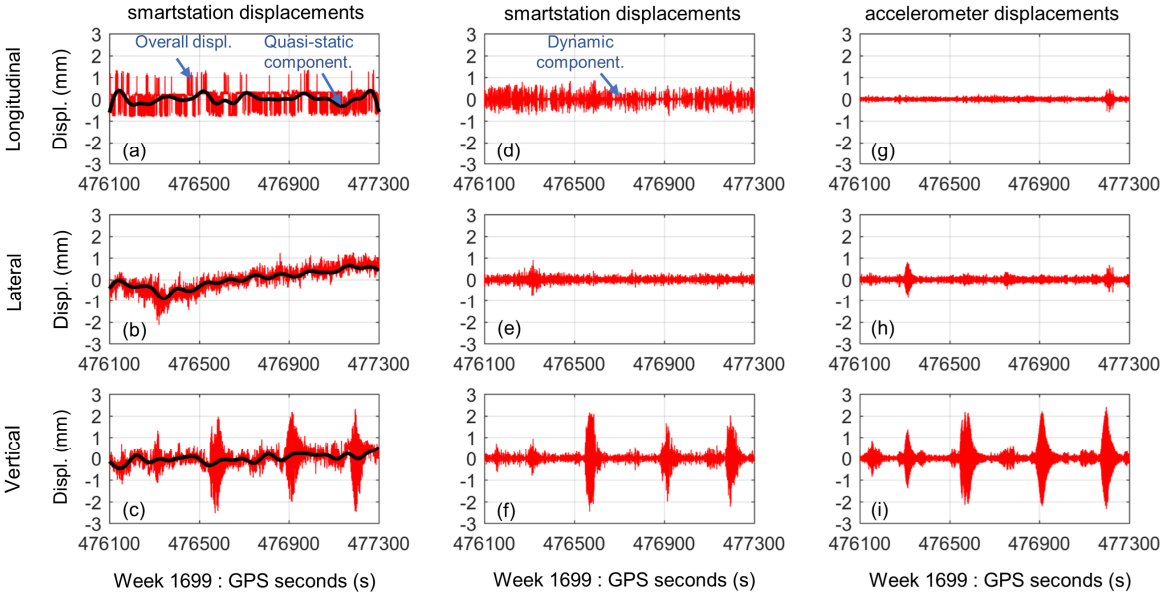
Figure 8. Time histories of displacements of the footbridge in three directions induced by gentle wind and the occasional pedestrian in experimental Case 3. The overall vibration displacements measured by the composite instrument (the red curves in the left column) were separated into two parts, i.e., the quasi-static displacements (the black curves in the left column) and dynamic displacements (central column). The dynamic displacements (right column) were also computed from the accelerometer data by double integration.

Figures 8a-c. graphically depict the overall vibration displacements of the footbridge in three directions measured by the composite instrument. They were preliminarily processed to remove

335 duplicates and outliers, and recover missing records as previously outlined above. All of these
336 displacements in three directions have small amplitudes with maximal amplitudes of 1.3 mm, 2.1
337 mm, and 2.5 mm in the longitudinal, lateral and vertical directions, respectively. It is obvious that the
338 composite instrument can sensitively identify the vibration displacements even though the vibration
339 displacements only have maximal amplitudes of about 2 mm.

340   Quasi-static displacements of the footbridge were also identified from the composite instrument
341 data, which are depicted by the black curves in the left column of Figure 8. They fluctuate within an
342 amplitude of 1 mm, which is usually caused by thermal expansion, wind, pedestrian-weight and so
343 on. Two sets of dynamic displacements of the footbridge in three directions were derived from both
344 the composite instrument and accelerometer data, which are depicted as shown in the central and
345 right columns of Figure 8, respectively. The dynamic displacements in each direction that were
346 derived from the composite instrument and accelerometer data are similar to each other. In the
347 vertical direction, the three peak values of the dynamic displacements derived from the composite
348 instrument data are about 2 mm, which agree well with those for the dynamic displacements derived
349 from the accelerometer data. This confirmed once again that the composite instrument can measure
350 dynamic displacements with maximum amplitudes of about 2 mm.

351   The modal frequencies of the footbridge in the vertical direction were identified using the fast
352 Fourier transform (FFT) method (Figure 9). Modal frequencies of 1.677 Hz and 2.885 Hz were detected
353 from the dynamic displacement time series of the composite instrument in the vertical direction. Also,
354 modal frequencies of 1.687 Hz and 2.875 Hz were detected from the dynamic displacement time series
355 of the accelerometer in the vertical direction. The difference in the values of the frequencies detected
356 from both the composite instrument and accelerometer are no more than 0.01 Hz, and the difference
357 ratio are less than 0.6 %. This shows that the composite instrument is capable of detecting relatively
358 low vibration frequencies of the footbridge.

359
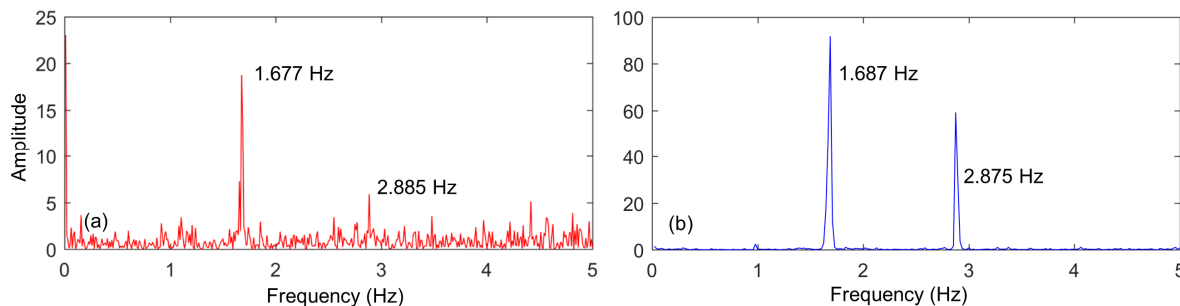
360 **Figure 9.** Comparison of FFT-based spectra of two dynamic displacements in the vertical direction:
361 (a) spectrum of the dynamic displacements derived from the composite instrument data, and (b) the
362 spectrum computed from the accelerometer data.
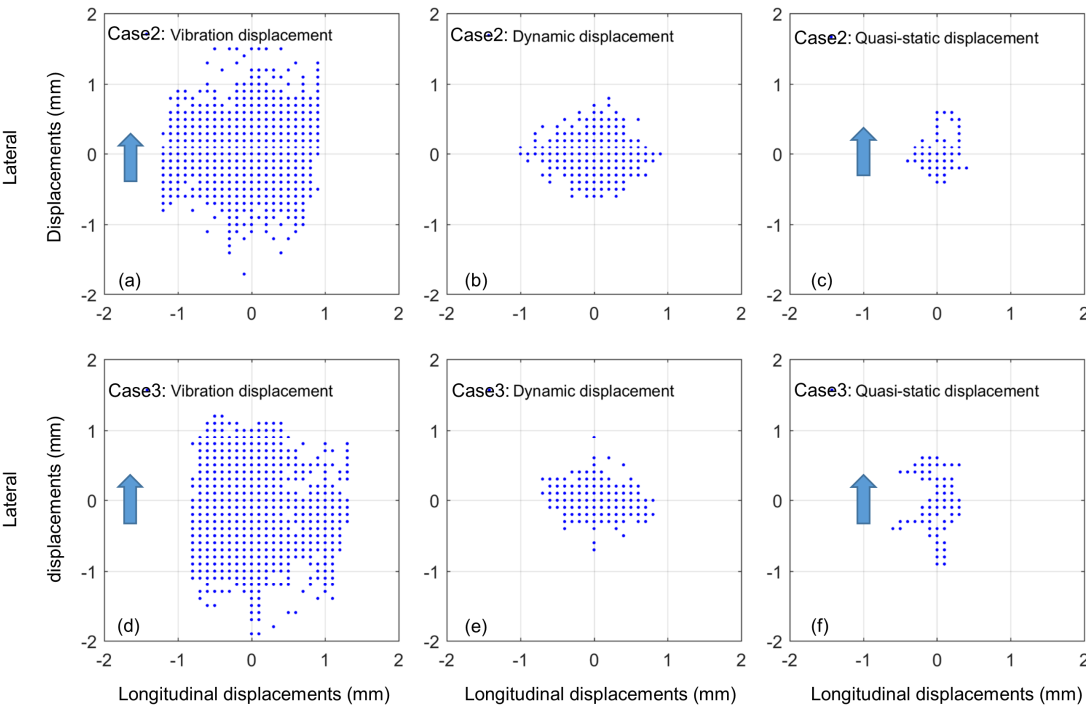
Figure 10. The distribution ranges of the longitudinal and lateral displacements of the measuring point of the studied footbridge, derived from the composite instrument measurements. The overall vibration displacements (**a**), dynamic displacements (**b**) and quasi-static displacements (**c**) in Case 2, and the corresponding ones (**d**, **e**, **f**) in Case 3. The distribution range of the overall vibration displacements in the lateral direction are significantly larger than the ones in the longitudinal direction as shown in subfigure (**a**). This is because the direction of the wind is along the lateral direction of the bridge, with blue arrows indicating the direction of the wind. Similar results can be found in subfigures (**c**), (**d**), and (**f**).

The distribution ranges of the longitudinal and lateral displacements of the measuring point of the footbridge are graphically depicted in Figure 10. These displacements were derived from the composite instrument data in experimental Case 2 and 3. In each case, the distribution range of the overall vibration displacements in the lateral direction are larger than the one in the longitudinal direction. The distribution range of the quasi-static displacements show similar characteristics. The reason is that the wind along the lateral directions causes relatively larger vibrations in the lateral direction, thus, the tendency for the increased displacements along the wind direction is evident.

5. Conclusions

A revolutionary surveying system using a composite instrument was proposed to monitor three-dimensional vibration displacements of a footbridge. Not only is it capable of detecting quasi-static and dynamic displacements of the footbridge, but it can also obtain nanosecond-level time information for each record, which is valuable for the fusion of multi-sensor data fusion. A CMWT algorithm was developed to understand the noise characteristics in the composite instrument measurements in the frequency domain. Experiments were conducted on the Nottingham Wilford Suspension Bridge to verify the measurements of vibration displacements of footbridges using the composite instrument. The Chebyshev highpass filter was adopted to separate quasi-static and dynamic displacements from the composite instrument measurements. Both wavelet and FFT algorithms were employed in the spectral analyses of the displacement time series in the frequency domain.

Firstly, we verified that the composite instrument possesses the capacity to accurately identify both quasi-static and dynamic displacements of footbridges with several millimeter amplitudes. The dynamic displacements created by three people jumping on the footbridge were identified by the

composite instrument, with displacement peak values from 5.7 to 10 mm. The accuracy of the measurement was superior to 1 mm. The quasi-static displacement components of the footbridge were identified from the composite instrument data with submillimeter-level accuracy. The corresponding peak differences between two sets of dynamic displacements derived from the composite instrument and accelerometer data are less than 1.0 mm and the peak difference ratios were no more than 10.0 %. In other case study, slight wind and occasional pedestrian-induced vibration displacements of the footbridge, with peak displacements from 1.3 to 2.5 mm, were accurately identified by the composite instrument. Relatively low vibration frequencies of 1.677 Hz and 2.885 Hz in the footbridge in the vertical direction, were identified from the composite instrument measurements.

The second contribution of this study is that the composite instrument measurement noise was characterized in detail by a CMWT algorithm in the frequency domain. All of the standard deviations of the background noise in each direction are no more than 0.5 mm when the composite instrument is 60 m away from the prism. The main noise energy is distributed within a relatively low frequency range of no more than 0.1 Hz.

The composite instrument could potentially be used as a tool for synchronously detecting the quasi-static and dynamic displacements of bridge structures with satisfactory accuracy. The study only concentrates on displacement monitoring of footbridges, but the composite instrument could be also used to identify the modal frequencies of footbridges, which would significantly improve its overall performance and data acquisition algorithm.

Author Contributions: Conceptualization, J.Y. and X.M.; methodology, J.Y.; software, J.Y.; validation, J.Y., Y.X. and Q.F.; formal analysis, J.Y.; investigation, J.Y., Q.F. and Z.F.; resources, J.Y.; data curation, J.Y.; writing—original draft preparation, J.Y.; writing—review and editing, Z.F.; visualization, J.Y.; supervision, X.M.; project administration, J.Y., X.M.; funding acquisition, J.Y. All authors have read and agreed to the published version of the manuscript.

Funding: This study is supported by the National Key R&D Program of China (No. 2016YFC0800207) and Changsha Science and Technology Project (No. kq1907110).

Acknowledgements: The University of Nottingham is thanked for supplying instruments in the field experiments.

Conflicts of Interest: The authors declare no conflicts of interest.

References

1. Esteban, V.B.G.; Gaxiola-Camacho, J.R.; Bennett, R.; Guzman-Acevedo, G.M.; Gaxiola-Camacho, I.E. Structural evaluation of dynamic and semi-static displacements of the Juarez Bridge using GPS technology. *Measurement* **2017**, *110*, 146–153.
2. Moschas, F.; Stiros, S. Dynamic Deflections of a Stiff Footbridge Using 100-Hz GNSS and Accelerometer Data. *J. Surv. Eng.* **2015**, *141*, 04015003.
3. Yi, T.H.; Li, H.N.; Gu, M. Experimental assessment of high-rate GPS receivers for deformation monitoring of bridge. *Measurement* **2013**, *46*, 420–432.
4. Shen, N.; Chen, L.; Liu, J.; Wang, L.; Tao, T.; Wu, D.; Chen, R. A Review of Global Navigation Satellite System (GNSS)-based Dynamic Monitoring Technologies for Structural Health Monitoring. *Remote Sens.* **2019**, *11*, 1001.
5. Yu, J.; Meng, X.; Yan, B.; Xu, B.; Fan, Q.; Xie, Y. Global Navigation Satellite System-based positioning technology for structural health monitoring: A review. *Struct. Contr. Health Monit.* **2020**, *27*, e2467.
6. Yang, J.; Li, J.; Lin, G. A simple approach to integration of acceleration data for dynamic soil–structure interaction analysis. *Soil Dyn. Earthquake Eng.* **2006**, *26*, 725–734.
7. Gindy, M.; Vaccaro, R.; Nassif, H.; Velde, J. A State-Space Approach for Deriving Bridge Displacement from Acceleration. *Comput. Aided Civ. Infrastruct. Eng.* **2008**, *23*, 281–290.
8. Ingensand, H.; Frei, E.; Scherrer, R. Scherrer, Surveying System Including an Electro-Optic Total Station and a Portable Receiving Apparatus Comprising a Satellite Position-Measuring System. Google Patents,

443 U.S. 5,233,357, 3 August 1993.

444 9. Biasion, A.; Cina, A.; Pesenti, M.; Rinaudo, F. An integrated GPS and Total Station instrument for cultural
445   heritage surveying: The LEICA SmartStation example. In Proceedings of the Cipa XX International
446   Symposium, Torino, Italy, 26 September–1 October 2005.

447 10. Leica. Leica SmartStation-Total Station with integrated GNSS, in Leica. 2019. Available online: https://leica-
448   geosystems.com/products/total-stations/systems/leica-smartstation (10th July 2020).

449 11. Cosser, E.; Roberts, G.W.; Meng, X.; Dodson, A. Measuring the dynamic deformation of bridges using a
450   total station. In Proceedings of the 11th FIG Symposium on Deformation Measurements, Santorini, Greece,
451   25 May 2003; Stiros, S., Pytharouli, S., Eds.; Geodesy and Geodetic Applications Lab., Patras Univ.: Patras,
452   Greece; pp. 605–612.

453 12. Erdogan, H.; Gülal, E. Ambient Vibration Measurements of the Bosphorus Suspension Bridge by Total
454   Station and GPS. *Exp. Tech.* **2013**, *37*, 16–23.

455 13. Psimoulis, P.A.; Stiros, S.C. Measuring Deflections of a Short-Span Railway Bridge Using a Robotic Total
456   Station. *J. Bridge Eng.* **2013**, *18*, 182–185.

457 14. Stiros, S.C.; Psimoulis, P.A. Response of a historical short-span railway bridge to passing trains: 3-D
458   deflections and dominant frequencies derived from Robotic Total Station (RTS) measurements. *Eng. Struct.*
459   **2012**, *45*, 362–371.

460 15. Moschas, F.; Stiros, S.C. Three-dimensional dynamic deflections and natural frequencies of a stiff
461   footbridge based on measurements of collocated sensors. *Struct. Control Health Monit.* **2013**, *21*, 23–42.

462 16. Lienhart, W.; Ehrhart, M.; Grick, M. High frequent total station measurements for the monitoring of bridge
463   vibrations. *J. Appl. Geod.* **2017**, *11*, 1–8.

464 17. Stiros, S.; Psimoulis, P.; Moschas, F.; Saltogianni, V.; Tsantopoulos, E.; Triantafyllidis, P. Multi-sensor
465   measurement of dynamic deflections and structural health monitoring of flexible and stiff bridges. *Bridge*
466   *Struct.* **2019**, *15*, 43–51.

467 18. Yu, J.; Meng, X.; Shao, X.; Yan, B.; Yang, L. Identification of Dynamic Displacements and Modal Frequencies
468   of a Medium-Span Suspension Bridge Using Multimode GNSS Processing. *Eng. Struct.* **2014**, *81*, 432–443.

469 19. Meo, M.; Zumpano, G.; Meng, X.; Cosser, E.; Roberts, G.; Dodson, A. Measurements of dynamic properties
470   of a medium span suspension bridge by using the wavelet transforms. *Mech. Syst. Signal Process.* **2006**, *20*,
471   1112–1133.

472 20. Chan, W.-S.; Xu, Y.-L.; Ding, X.; Xiong, Y.-L.; Dai, W.-J. Assessment of Dynamic Measurement Accuracy of
473   GPS in Three Directions. *J. Surv. Eng.* **2006**, *132*, 108–117.

474 21. Yu, J.; Zhu, P.; Xu, B.; Meng, X. Experimental assessment of high sampling-rate robotic total station for
475   monitoring bridge dynamic responses. *Measurement* **2017**, *104*, 60–69.

476 22. Cazelles, B.; Chavez, M.; De Magny, G.C.; Guegan, J.-F.; Hales, S. Time-dependent spectral analysis of
477   epidemiological time-series with wavelets. *J. R. Soc. Interface* **2007**, *4*, 625–636.

478 23. Yu, J.; Yan, B.; Meng, X.; Shao, X.; Ye, H. Measurement of Bridge Dynamic Responses Using Network-Based
479   Real-Time Kinematic GNSS Technique. *J. Surv. Eng.* **2016**, *142*, 04015013.

480 24. Roberts, G.; Meng, X.; Dodson, A.H. Integrating a Global Positioning System and Accelerometers to
481   Monitor the Deflection of Bridges. *J. Surv. Eng.* **2004**, *130*, 65–72.

482 25. Wang, J.; Meng, X.; Qin, C.; Yi, J. Vibration Frequencies Extraction of the Forth Road Bridge Using High
483   Sampling GPS Data. *Shock. Vib.* **2016**, *2016*, 1–18.

484 26. Meng, X.; Dodson, A.; Roberts, G. Detecting bridge dynamics with GPS and triaxial accelerometers. *Eng.*
485   *Struct.* **2007**, *29*, 3178–3184.

486 27. Park, K.-T.; Kim, S.-H.; Park, H.-S.; Lee, K.-W. The determination of bridge displacement using measured
487   acceleration. *Eng. Struct.* **2005**, *27*, 371–378.

488 28. Kim, K.; Choi, J.; Chung, J.; Koo, G.; Bae, I.-H.; Sohn, H. Structural displacement estimation through multi-
489   rate fusion of accelerometer and RTK-GPS displacement and velocity measurements. *Measurement* **2018**,
490   *130*, 223–235.

491

492